



# Preparation of graphene oxide composited zinc oxide films by electrostatic spray deposition for humidity sensors

Thitiwat Maboonchauy, Korakot Onlaor, Thutiyaporn Thiwawong\*, Benchapol Tunhoo

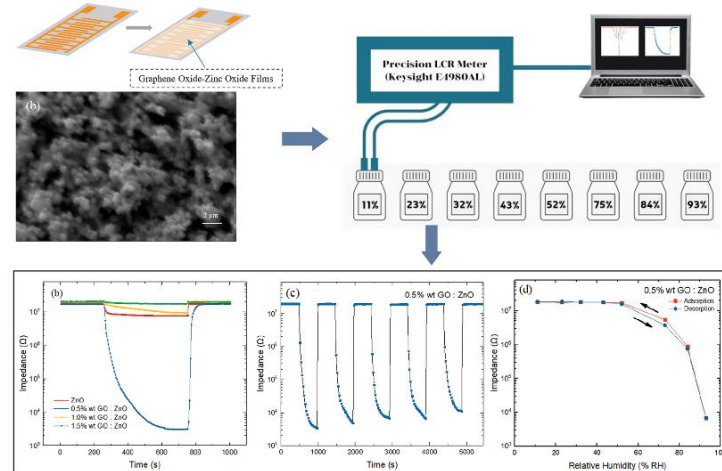
Electronics and Control Systems for Nanodevices Research Laboratory,  
College of Materials Innovation and Technology, King Mongkut's Institute of Technology Ladkrabang,  
Chalongkrung Road, Bangkok, 10520 Thailand

\*Corresponding Author: thutiyaporn.th@gmail.com  
<https://doi.org/10.55674/jmsae.v11i3.252232>

Received: 6 September 2022 | Revised: 9 September 2022 | Accepted: 15 March 2023 | Available online: 1 September 2023

## Abstract

This work aimed to study the preparation of graphene oxide (GO) and zinc oxide (ZnO) composited films by electrostatic spray deposition for use in fabricated humidity sensors. The physical properties of prepared films were examined with X-ray diffraction, Raman spectroscopy, and scanning electron microscope. Subsequently, a humidity sensor was fabricated using a low-cost interdigitated electrode pattern with the print circuit board. The humidity sensing behaviors were assessed with fixed humidity levels in a saturated aqueous salt solution in the humidity range of 11 – 93%RH. The impedance value of the device was obtained with a precision LCR meter. It was found that the composited film of 0.50 %wt. GO demonstrated the highest humidity response with optimized humidity sensitivity, hysteresis error, and response/recovery times of  $2.68 \times 10^3$ , 4.89%, and 228/19 s, respectively. Moreover, the equivalent circuits for the prepared device at various humidity levels were acquired with impedance spectroscopy to propose the mechanism for the humidity sensing of the device.



**Keywords:** Humidity sensor; ZnO; Graphene oxide

© 2023 Center of Excellence on Alternative Energy reserved

## Introduction

Humidity is an important physical value for environmental properties. Generally, the captured water vapor in the air resulted in a term of moisture for humidity value. The humidity level plays a significant role in many operations, such as electronic storage, pharmaceutical, and industrial applications. Therefore, the measurement of humidity levels is crucial. Humidity sensors are widely used to gauge the humidity level and can be prepared from various materials such as metal oxide [1], the polymer [2], carbon-based materials [3], etc. One of the most interesting materials used in fabricated humidity devices is nanomaterials.

Nanomaterials are the focus of fields of emerging material. Due to their exhibits more advantages properties

such as simple process, low cost, high performance, etc. Zinc oxide (ZnO) is a crucial material with outstanding properties [1], such as direct energy band gap, good electron transport behavior, etc. Thus, ZnO has been studied extensively and used in various applications, including sensors [4], photodetectors [5], light-emitting devices [6], and solar cells [7]. Several processes using diverse physical and chemical methods can be used to synthesize ZnO material. The prepared process parameters tend to be affected by the properties of the synthesized particles. Usually, ZnO material can be used in the humidity device. Sensing properties have depended on pristine material properties, which can be modified with additive materials such as doping or composite [8 – 10].

Graphene is well known as one layer of atomically carbon  $sp^2$  bonding material with a honeycomb structure [11]. Graphene oxide (GO) is a derivative graphene material with attached functional groups (=O, -OH, etc.) on graphene sheets. The attached functional groups influence the solubility and dispersibility of GO in various solvents [12, 13]. The surface properties of GO material represent the hydrophilicity behavior, which favoured the moisture molecule absorption [14]. Moreover, the functional groups of GO can absorb the moisture molecules around the environment, making it applicable as a candidate for humidity sensor devices [15].

Electrostatic spray deposition is a facile technique for the preparation of nanomaterials. Various kinds of nanomaterials, such as metal nanoparticles and metal oxide films, can be deposited using this technique [16]. The ESD technique enables certain advantages such as low-cost and non-complicated systems, as well as easy control of the behaviors of prepared films and the non-vacuum requirement for preparation systems. Consequently, ESD has been applied to fabricate many electronic devices such as sensors, photovoltaic cells, and energy storage devices [17]. The basic operation of the ESD technique is the generation of fine droplets of precursor solution with applied high voltage. Fine droplets are accumulated on a substrate to form a prepared film. The influence of preparation parameters such as high voltage level, precursor flow rate, and substrate temperature affect the properties of deposited films.

For enhances of materials performance, the composite of ZnO and GO has attracted interest due to their beneficial properties. The ZnO-GO composite demonstrates the potential for various properties. Mei [18] reported the sunlight-catalytic performance of composite GO and ZnO materials. The performance of photocatalytic was enhanced in the composited material. Paul [19] reported on enhancing UV detection in the GO/ZnO composite thin films. Due to the defect state modulation and the carrier density was improved in composite thin films. Tao [20] reported the humidity sensor performance based on GO/ZnO/plant cellulose film. The sensing layer of GO/ZnO films was prepared by hydrothermal process. The device exhibited high performance for use as a sensor for respiratory monitoring systems. Typically, the composite GO, and ZnO can be prepared by various methods such as sol-gel, hydrothermal, etc. So, those methods cannot be used to prepare composite films on flexible or plastic substrates. Therefore, this work presents the application of the electrostatic spray deposition technique to deposit GO and

ZnO composite film on the plastic substrate.

In this work, GO and ZnO composite films were deposited by electrostatic spray deposition. The influence of GO composition on the properties of composite films was examined, and the humidity sensing of composite GO and ZnO films was investigated. Moreover, the mechanism of humidity sensing for the prepared device was established with impedance spectroscopy.

## Materials and Methods

The waste cow's research process (Fig. 1) was processed ZnO nanoparticles were synthesized by co-precipitation with an aqueous precursor of 0.40 M  $Zn(NO_3)_2$  and 4 M KOH. Both solutions were mixed at a temperature of 60 °C with magnetic stirring at 100 rpm. The resulting white particles were collected and washed with DI water several times. The final powder was dried in an oven at 70 °C to get the ZnO nanoparticles, and the GO particles were prepared using a modified Hummer method [21]. Briefly, the graphite powder was oxidized with  $H_2SO_4$ ,  $NaNO_3$ , and  $KMnO_4$ , while  $H_2O_2$  and DI were used to stop the reaction, thus obtaining synthesized graphene oxide. Before that, the GO and ZnO nanoparticles at various compositions were mixed in ethanol with a 100 mg  $ml^{-1}$  concentration, which was used as starter material. The lab-made electrostatic spray deposition (ESD) technique was used to deposit GO, and ZnO composited films. Fig. 1(a) depicts the experimental setup of the ESD system, in which the stater material was fed from a syringe pump to deposit film onto the substrate. A syringe pump (NE1000) fed the starter material contained in a plastic syringe with a stainless nozzle to deposit the composited films. The parameters for ESD deposition, including precursor flowrate, a dc applied voltage, the distance of the metal nozzle to film substrate, and deposition time, were maintained at 0.50  $ml\ hr^{-1}$ , 10 kV, 4 cm, and 10 min, respectively. The substrate for prepared films was soda-lime glass. The physical properties of composited films were investigated by X-ray diffraction (Rigaku, SmartLab), Raman spectrophotometer (DXR Smart Raman), and scanning electron microscopy (Zeiss, EVO 15), respectively. A humidity sensor can be fabricated using a low-cost interdigitated electrode pattern with a printed circuit board. Aqueous saturated salt solutions of  $LiCl$ ,  $CH_3COOK$ ,  $MgCl_2$ ,  $K_2CO_3$ ,  $Mg(NO_3)_2$ ,  $NaCl$ ,  $KCl$ , and  $KNO_3$  in closed glass vessels were used at humidity value measurements of 11, 23, 32, 43, 53, 75, 84, and 93 %RH, respectively. The fabricated device was stored in each vessel of humidity values, and the impedance characteristics were measured using a precision LCR meter (Keysight,

E4980AL) with a program on computer control. Fig. 1(b) illustrates the humidity measurement setup diagram. Moreover, the sensing mechanism for the fabricated device was obtained with impedance spectroscopy. The impedance characteristics were presented with a frequency range of 20 Hz – 1 MHz. The equivalent circuits for the device were proposed.

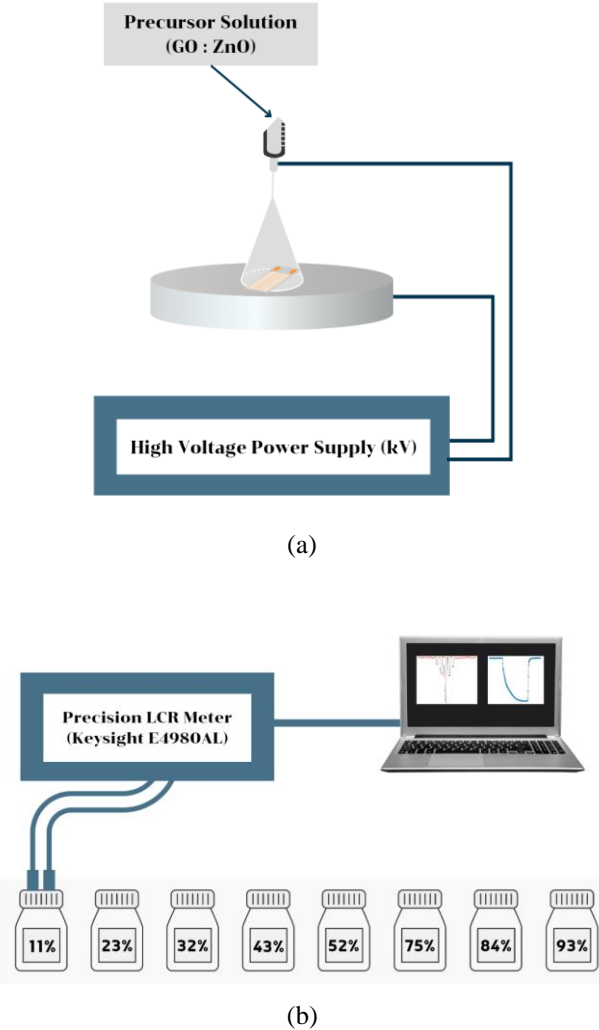


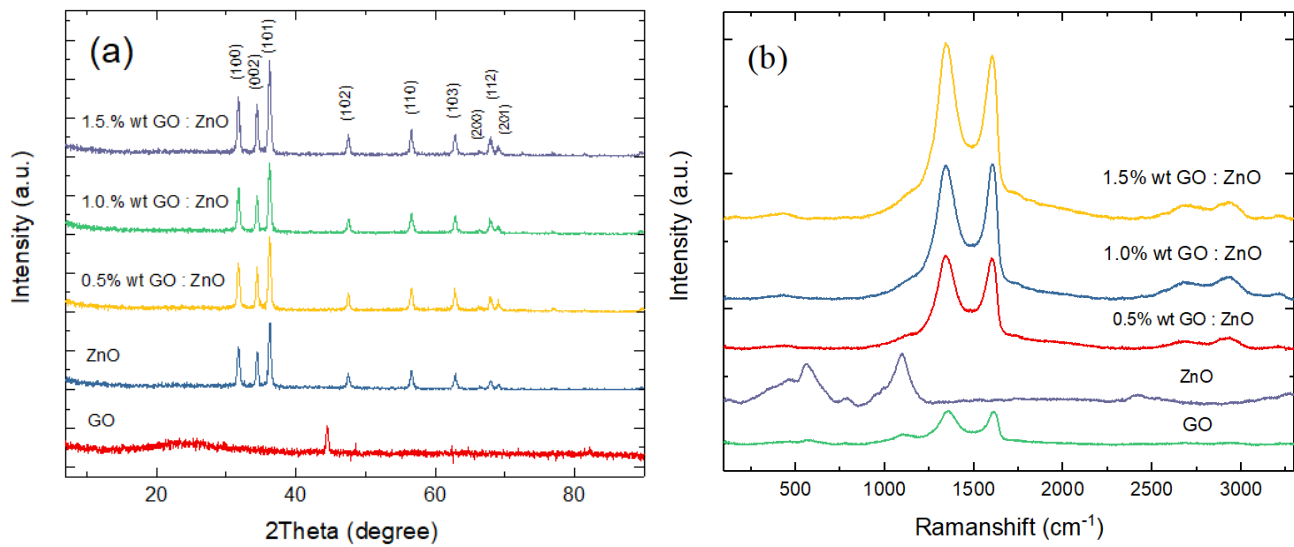
**Fig. 1** (a) the experimental setup of the electrostatic spray deposition system, (b) humidity measurement system diagram.

## Results and Discussions

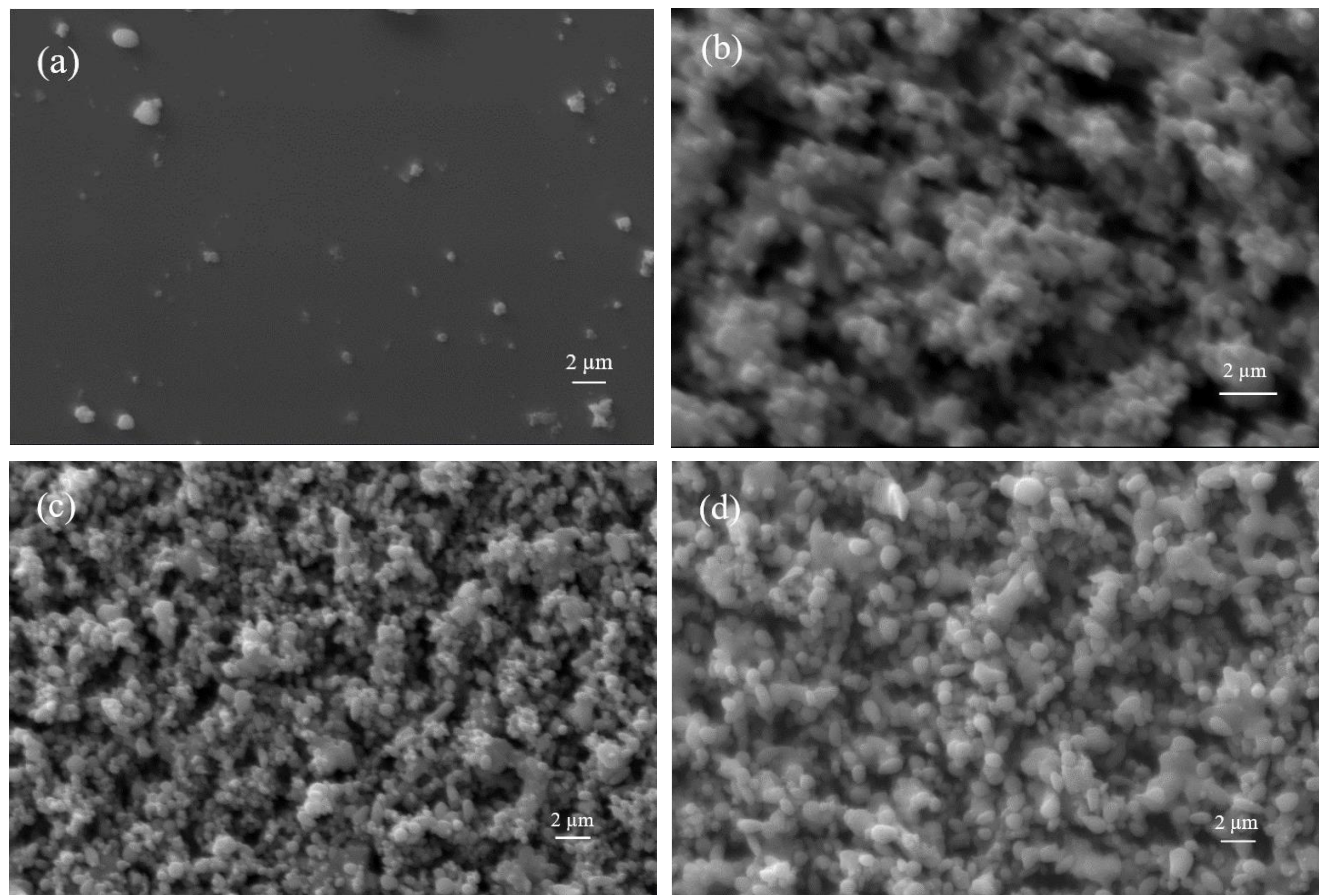
The XRD patterns for composited GO and ZnO films are shown in Fig. 2. In the case of ZnO nanoparticle film, the

dominant diffraction pattern of (100), (002), (101) planes at diffraction peaks ( $2\theta$ ) of 31.80, 34.40, and 36.20 deg. (JCPDS No. 80-0075) were found [22], which can be indicated by the crystalline orientation plane of the hexagonal structure. Moreover, subtle diffraction peaks at 47.60, 56.70, 62.90, and 68.10 deg. corresponded with orientation planes of (102), (110), (103), and (112), respectively, for hexagonal ZnO. Thus, the XRD results indicate the formation of c-axis hexagonal ZnO nanoparticles. For the structure of GO, a broadening peak at a diffraction angle of approximately 24 – 25 deg. can be seen. In another report [23], this broadening diffraction peak can be assigned as the (002) orientation plane of graphene oxide material with an interlayer spacing of 4 Å. Usually, the GO was composed of graphene sheets with intercalated functional groups between stack layers of graphene sheets. Therefore, the increment of interplanar spacing resulted in the broadening XRD peak. Moreover, a broadening peak might also affect the disorder in stacking graphene oxide sheets. The prominent peaks of ZnO nanoparticles were observed for the diffraction patterns of composite GO and ZnO nanoparticles because the diffraction peak of GO is difficult to observe.

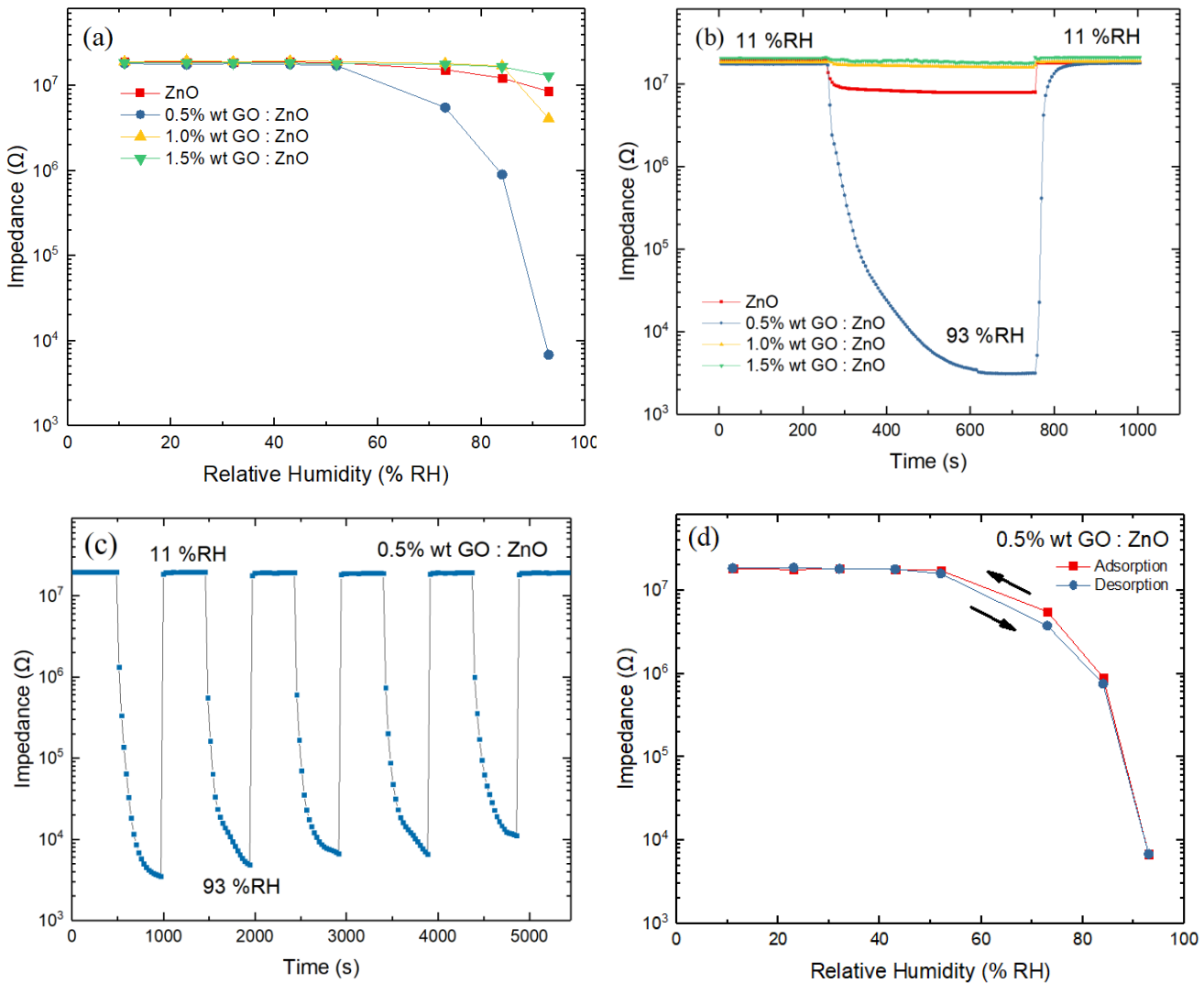
Raman spectroscopy is a common tool used to identify the structural characteristics of prepared composite films. The Raman spectra of GO can be demonstrated at 1300 and 1580  $\text{cm}^{-1}$ , which are the D and G bands of carbon material, respectively. Typically, the G-band is the Raman active for carbon  $\text{sp}^2$  hybridized bonding, and the D-band is the defect band for GO material [24]. For the Raman spectra of ZnO, the prominent peak is observed at 1,151  $\text{cm}^{-1}$ , which is the ZnO  $\text{E}_1(\text{LO})$  phonon mode [25]. In the case of composite GO and ZnO nanoparticle films, it was found that the Raman spectra of GO were largely dominant until they covered up other signals of ZnO spectra. At the same time, the subtle Raman peak of ZnO can be observed at 1,151  $\text{cm}^{-1}$  as the shoulder position of D-band GO. However, the XRD and Raman results confirmed the composite film formation of GO and ZnO. The surface morphologies of ESD films made of composite GO: ZnO is illustrated in Fig. 3. It can be seen that the particle-like morphology due to the start of ESD preparation comprised nanoparticles dispersed in an ethanol solvent without post-thermal treatment. In addition, this process can be used to prepare films on flexible substrates such as plastic or paper.



**Fig. 2** (a) XRD pattern and (b) Raman spectra of GO composite ZnO nanoparticles films.



**Fig. 3** Surface morphologies of GO composite ZnO nanoparticles films at various concentrations of (a) ZnO, (b) 0.50% GO, (c) 1% GO, and (d) 1.50% GO.



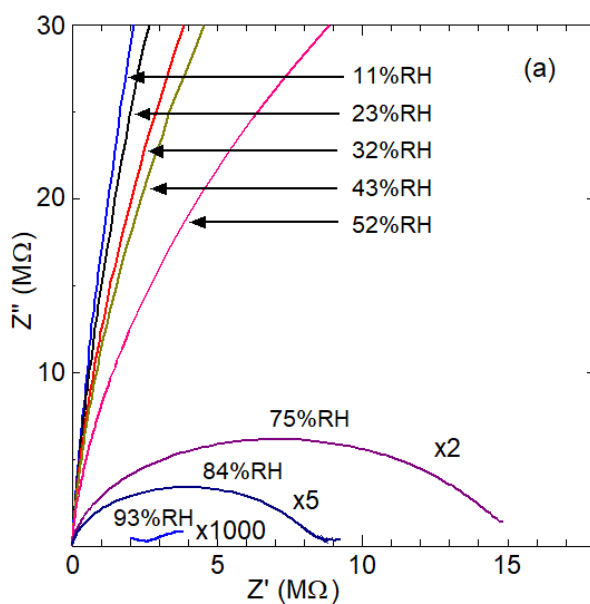
**Fig. 4** (a) Humidity sensitivity, (b) response-recovery times, (c) repeatability response between 11 – 93 % RH and (d) hysteresis characteristic.

Fig. 4(a) depicts the fabricated device humidity response at various GO compositions. The inset of Fig. 4(a) exhibits the response of the fabricated sensor during measurement at various humidity levels and measurement times. The impedance of the fabricated device exhibited high impedance values at low humidity levels, which decreased at high humidity levels. It was due to the influence of moisture capture on the surface of composites films. It was found that the device with 0.50% wt. of GO has demonstrated the highest humidity response with a sensitivity of  $2.68 \times 10^3$  in a humidity range of 11 – 93%RH.

Typically, GO is a natural hydrophilic behavior. Thus, humidity sensing can be improved with the composite of GO

in ZnO films. The optimum sensitivity was found with 0.50% wt of GO. With the increasing GO loading in composite films, the performance of the device is improved. The sensitivity decrease might be due to the diminishing of active sites for humidity sensing. This behavior was found in other composite GO materials.[26, 27]

The device time response characteristics were evaluated with the device response behaviors between humidity values of 11%RH and 93 %RH, as shown in Fig. 4(b). The optimum time response for the device was observed with 0.50% wt of GO. The response and recovery times could be performed in approximately 228 s and 19 s, respectively. More discussion will be expanded and described later in complex impedance measurements.

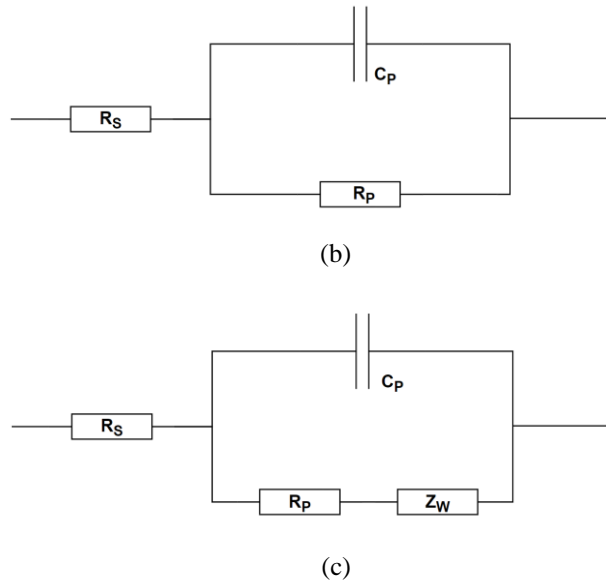


**Fig. 5** (a) Cole-Cole plot (b) an equivalent circuit in a low humidity range, and (c) an equivalent circuit in a high humidity range.

In addition, the repeatability of the device was tested with repeated measurement sequences between humidity levels of 11%RH and 93%RH for five cycles, as shown in Fig. 4(c). The results exhibited the stability of the device under repeatability testing. Fig. 4(d) shows the hysteresis error of the prepared device with 0.50% wt. GO: ZnO films. The hysteresis error ( $\gamma_H$ ) can be estimated from  $\gamma_H = \pm(1/2)(\Delta H_{\max}/F_{FS})$  [28], where  $F_{FS}$  is the full-scale output, and  $\Delta H_{\max}$  is the output at the largest difference in forward and backward measurement. The maximum hysteresis error is 4.89% at a humidity of 75 %RH. The cause of the hysteresis error might be due to the imperfect sensing characteristics from the swelling of moisture molecules in sensing material between adsorption and desorption processes [20]. Typically, the adsorption and desorption mechanisms differ from the influence of the adsorption of the capillary moisture molecule [29]. The humidity response relied on the imbalance between the capture and release of the capillary moisture molecule.

Complex impedance spectroscopy is a versatile method used to scrutinize the mechanism of an electronic device. The technique can be used in many applications. Typically, complex impedance is composed of a real part ( $Z'$ ) and an imaginary part ( $Z''$ ) derived from the measured impedance and phase difference values. The plot of  $Z'$  versus  $Z''$  is called the Cole-Cole plot. Fig. 5 depicts the Cole-Cole plot of 0.50 %wt. GO: ZnO fabricated humidity sensor at various

humidity values from 11 – 93 %RH. In low humidity ranges,



a semicircle graph shape can be seen. With increased humidity levels, the graph shapes comprise a semicircle graph with a linear tail line. Fig. 5(b) and 5(c) show equivalent circuits for low and high humidity regimes. Typically, the humidity sensing mechanism depends on water molecule adsorption on the material surface. The sensing mechanism of the humidity sensor is based on the two mechanisms regimes. In a low humidity regime, the moisture molecules were low. Thus, adsorption is the bonding between vapor moisture molecules and various sites, such as functional groups or vacancies of the sensing surface. The movement of moisture molecules is low with the influence of double hydrogen bonding between moisture molecules and the sensing layer, which results in low conductivity or high impedance value, as shown in Fig. 4(a). The dominant charge transfer was the hopping mechanism between neighborhood sites. So, the large intrinsic resistance of prepared films is dominant.

Moreover, in high humidity regime, the vapor moisture ions are more adsorbed on the surface of the sensing material with multilayer physisorption. Sequentially, the higher moisture molecules formed the multilayer of physisorption. The moisture molecules were bonded with single hydrogen bonding in the multilayers forming, resulting in the nearly free residue charge on the surface. The results of the surface charge are easy to transport. At the same time, the increasing

electrolytic conduction over the sensing layer reduces the semicircle graph of the Cole-Cole plot. In this regime, the physisorption molecule layers act as the liquid-like layer in which the charge in multilayers formed was the formation of hydronium ions ( $\text{H}_3\text{O}^+$ ) due to the ionized moisture molecules with an electrostatic force. The hydronium ions can generate conductivity in the device explained by the Grothuss chain reaction ( $\text{H}_2\text{O} + \text{H}_3\text{O}^+ \rightleftharpoons \text{H}_3\text{O}^+ + \text{H}_2\text{O}$ ) [30, 31]. Thus, the impedance of the device decreased when increasing the humidity levels. Commonly, the semicircle graph of the Cole-Cole plot is related to the sensing behaviors of the humidity sensor, which can be expressed as primary components of resistance and capacitance. The significant intrinsic resistance was found at low humidity regimes due to the low conductivity. Whereas, in high humidity regime, more charge carriers occurred with high conductivity due to the influence of multilayer physisorption. Therefore, the decreasing of semicircles graphs is found. Moreover, in high humidity regime, a Warburg component represents the effect of the diffusion and intercalation of moisture ions into the interlayer of the sensing material.

## Conclusion

An electrostatic spray deposition technique with starter materials of nanoparticles can prepare the composite films of graphene oxide and zinc oxide. The effect of GO concentration on the properties of prepared composite films was performed by XRD, Raman spectroscopy, and scanning electron microscope. The XRD results exhibited the dominant diffraction peaks of ZnO and the broadening peak of GO. The Raman spectra can be used to identify the characteristics of ZnO and GO materials. The surface morphology depicted the fine nanoparticles over the surface of composite films. The fabricated device exhibited the maximum humidity sensitivity of 0.50% wt. of GO in the humidity region between 11 – 93%RH. The maximum hysteresis error of the device, response, and recovery time are 4.89%, 228 s, and 19 s, respectively. The sensing mechanisms of the device can be performed with the Cole-Cole plot of impedance spectroscopy. This can explain the dominant mechanism of physisorption in the lower regime of humidity level and chemisorption in the high level.

## Acknowledgement

This work was supported financially with a research fund by King Mongkut's Institute of Technology Ladkrabang (KMITL grant number: RE-KRIS/FF65/39).

The authors acknowledge the facilities and technical assistance received from the Nanotechnology and Materials Analytical Instrument Service Unit (NMIS) of the College of Materials Innovation and Technology, King Mongkut's Institute of Technology Ladkrabang.

## References

- [1] L. Gu, K. Zheng, Y. Zhou, J. Li, X. Mo, G. R. Patzke, G. Chen, Humidity sensors based on  $\text{ZnO}/\text{TiO}_2$  core/shell nanorod arrays with enhanced sensitivity, *Sens. Actuators B Chem.* 159(1) (2011) 1 – 7.
- [2] W. Yao, X. Chen, J. Zhang, A capacitive humidity sensor based on gold-PVA core-shell nanocomposites. *Sens. Actuators B Chem.* 145(1) (2010) 327 – 333.
- [3] H. -W. Yu, H. K. Kim, T. Kim, K. M. Bae, S. M. Seo, J.-M. Kim, T. J. Kang, Y. H. Kim, Self-Powered Humidity Sensor Based on Graphene Oxide Composite Film Intercalated by Poly(Sodium 4-Styrenesulfonate), *ACS Appl. Mater. Interfaces*. 6(11) (2014) 8320 – 8326.
- [4] Z. Lin, F. Guo, C. Wang, X. Wang, K. Wang, Y. Qu, Preparation and sensing properties of hierarchical 3D assembled porous ZnO from zinc hydroxide carbonate, *RSC Adv.* 4(10) (2014) 5122 – 5129.
- [5] A. Manekkathodi, M. -Y. Lu, C. W. Wang, L. -J. Chen, Direct Growth of Aligned Zinc Oxide Nanorods on Paper Substrates for Low-Cost Flexible Electronics, *Adv. Mater.* 22(36) (2010) 4059 – 4063.
- [6] R. Könenkamp, R. C. Word, C. Schlegel, Vertical nanowire light-emitting diode, *Appl. Phys. Lett.* 85(24) (2004) 6004 – 6006.
- [7] J. B. Baxter, E. S. Aydil, Nanowire-based dye-sensitized solar cells, *Appl. Phys. Lett.* 86(5) (2005) 053114.
- [8] S.-P. Chang, S. -J. Chang, C.-Y. Lu, M. -J. Li, C. -L. Hsu, Y. -Z. Chiou, T. -J. Hsueh, I. -C. Chen, A ZnO nanowire-based humidity sensor, *Superlattices and Microstruct.* 47(6) (2010) 772 – 778.
- [9] R. Zhang, P.-G. Yin, N. Wang, L. Guo, Photoluminescence and Raman scattering of ZnO nanorods, *Solid State Sci.* 11(4) (2009) 865 – 869.
- [10] A. Ismail, M. Mamat, N. Md, Fabrication of hierarchical Sn-doped ZnO nanorod arrays through sonicated sol-gel immersion for room temperature, resistive-type humidity sensor applications, *Ceram. Int.* 42(8) (2016) 9785 – 9795.

[11] Y. Yao, X. Chen, H. Guo, Z. Wu, Graphene oxide thin film coated quartz crystal microbalance for humidity detection, *Appl. Surf. Sci.* 257(17) (2011) 7778–7782.

[12] A. Chavez-Valdez, M. S. P. Shaffer, A. R. Boccaccini, Applications of Graphene Electrophoretic Deposition, A Review. *J. Phys. Chem. B.* 117(6) (2013) 1502–1515.

[13] S. ParkR. S. Ruoff. Chemical methods for the production of graphenes. *Nat. Nanotechnol.* 4(4) (2009) 217–224.

[14] H. Bi, K. Yin, X. Xie, J. Ji, S. Wan, L. Sun, M. Terrones, M. S. Dresselhaus, Ultrahigh humidity sensitivity of graphene oxide, *Sci. Rep.* 3(1) (2013) 2714.

[15] S. Borini, R. White, D. Wei, M. Astley, S. Haque, E. Spigone, N. Harris, J. Kivioja, T. Ryhänen, Ultrafast Graphene Oxide Humidity Sensors, *ACS Nano.* 7(12) (2013) 11166–11173.

[16] M. Cloupeau, B. Prunet-Foch, Electrohydrodynamic spraying functioning modes: a critical review. *J. Aerosol Sci.* 25(6) (1994) 1021–1036.

[17] D. Kang, J. Kim, I. Kim, K.-H. ChoiT.-M. Lee. Experimental Qualification of the Process of Electrostatic Spray Deposition, *Coat.* 9(5) (2019) 294.

[18] W. Mei, M. Lin, C. Chen, Y. Yan, L. Lin, Low-temperature synthesis and sunlight-catalytic performance of flower-like hierarchical graphene oxide/ZnO macrosphere, *J. Nanopart Res.* 20 (2018) 1–12.

[19] R. Paul, R. Gayen, S. Biswas, S. V. Bhat, R. Bhunia, Enhanced UV detection by transparent graphene oxide/ZnO composite thin films, *RSC Adv.* 6(66) (2016) 61661–61672.

[20] B. Tao, J. Yin, F. Miao, Y. Zang, High-performance humidity sensor based on GO/ZnO/plant cellulose film for respiratory monitoring, *Ionics.* 28(5) (2022) 2413–2421.

[21] P. Songkeaw, B. Tunhoo, T. Thiawong, K. Onlaor, Transparent write-once-read-many-times memory devices based on an ITO/EVA:rGO/ITO structure, *J. Mater. Sci.: Mater. Electron.* 29(20) (2018) 17517–17524.

[22] N. T. Shimpi, Y. N. Rane, D. A. Shende, S. R. Gosavi, P. B. Ahirrao, Synthesis of rod-like ZnO nanostructure: Study of its physical properties and visible-light driven photocatalytic activity, *Optik.* 217(2020) 164916.

[23] P. Songkeaw, K. Onlaor, T. Thiawong, B. Tunhoo, Reduced graphene oxide thin film prepared by electrostatic spray deposition technique, *Mater. Chem. Phys.* 226(2019) 302–308.

[24] L. G. Cançado, A. Jorio, E. H. M. Ferreira, F. Stavale, C. A. Achete, R. B. Capaz, M. V. O. Moutinho, A. Lombardo, T. S. Kulmala, A. C. Ferrari, Quantifying Defects in Graphene via Raman Spectroscopy at Different Excitation Energies, *Nano Lett.* 11(8) (2011) 3190–3196.

[25] C. V. V. Ramana, M. K. Moodely, V. Kannan, A. Maity, J. Jayaramudu, W. Clarke, Fabrication of stable low voltage organic bistable memory device, *Sens. Actuators B Chem.* 161(1) (2012) 684–688.

[26] W. -D. Lin, C. -T. Liao, T. -C. Chang, S. -H. Chen, R. -J. Wu, Humidity sensing properties of novel graphene/TiO<sub>2</sub> composites by sol–gel process, *Sens. Actuators B Chem.* 209 (2015) 555–561.

[27] A. Subki, M. H. b. Mamat, M. Musa, M. Abdullah, I. S. Banu, N. Vasimalai, M. Ahmad, N. Nafarizal, A. Suriani, A. Mohamad, Effects of varying the amount of reduced graphene oxide loading on the humidity sensing performance of zinc oxide/reduced graphene oxide nanocomposites on cellulose filter paper, *J. Alloys Compd.* 926 (2022) 166728.

[28] T. Thiawong, K. Onlaor, B. Tunhoo, A Humidity Sensor Based on Silver Nanoparticles Thin Film Prepared by Electrostatic Spray Deposition Process, *Adv. Mater. Sci. Eng.* 2013(2013) 640428.

[29] G. Korotcenkov, N. P. Simonenko, E. P. Simonenko, V. V. Sysoev, V. Brinzari, Based Humidity Sensors as Promising Flexible Devices, State of the Art, Part 2: Humidity-Sensor Performances. *Nanomaterials.* 13(8) (2023) 1381.

[30] A. Tripathy, S. Pramanik, A. Manna, S. Bhuyan, N. F. Azrin Shah, Z. Radzi, N. A. Abu Osman, Design and Development for Capacitive Humidity Sensor Applications of Lead-Free Ca, Mg, Fe, Ti-Oxides-Based Electro-Ceramics with Improved Sensing Properties via Physisorption, *Sens.* 16(7) (2016) 1135.

[31] N. Li, X. Chen, X. Chen, X. Ding, X. Zhao, Ultrahigh humidity sensitivity of graphene oxide combined with Ag nanoparticles, *RSC Adv.* 7(73) (2017) 45988–45996.